# Measurement of Discrete Gamma-ray Production Cross Sections for Interactions of 14 MeV Neutron with Mg, Al, Si, Ti, Fe, Ni, Cu, Nb, Mo and Ta

Hitoshi Sakane[*], Yoshimi Kasugai[**], Fujio Maekawa[**],
Yujiro Ikeda[**] and Kiyoshi Kawade[*]
*Energy Engineering and Science, Nagoya University,
Furo-cho, Chikusa-ku, Nagoya 464-8603
*e-mail:* sakane@fnshp.tokai.jaeri.go.jp
**Japan Atomic Energy Research Institute,
Tokai-mura, Naka-gun, Ibaraki-ken 319-1195

We started to measure systematically discrete gamma-ray production cross sections by 14 MeV DC neutron beam. Measured targets were Mg, Al, Si, Ti, Fe, Ni, Cu, Nb, Mo and Ta. Some discrete gamma-ray production cross section data for these targets were newly obtained. The data for Ta were obtained for the first time. The experimental efficiency attained by the use of the method was about 50 times larger than the general experiments using pulsed neutrons. In result, good statistic data could be obtained in a short span of time.

## 1 Introduction

Gamma-ray production cross sections for 14 MeV neutrons are of importance not only for radiation shielding designs of nuclear facilities but also for evaluation of gamma-ray heating of fusion reactors. Besides the practical importance, discrete gamma-ray spectra and production cross sections are required to understand the nuclear structure and the neutron reaction mechanism. However accurate experimental data have not been measured sufficiently or there are no available data for some specific materials, because a suitable experimental environment has been limited. Thus, we started to measure systematically discrete gamma-ray production cross sections for 14 MeV neutrons. For the measurement, a high performance collimator system was installed at FNS to extract 14 MeV neutron beam.

## 2 Experiment

The experimental arrangement is shown in Fig. 1. The main collimator was composed of a Fe block 120 cm thick, a polyethylene block 40 cm thick, a Cd sheet 1mm thick and a Pb block 20 cm thick, and the pre-collimator was composed of a Fe block 50 cm thick.

The diameter of collimator was 2 cm. The angle between the deuteron beam and the axis of the collimated neutron beam was 80 degree, which resulted in a 14.2 MeV neutron energy. The absolute neutron flux was determined by the $^{27}Al(n,\alpha)^{24}Na$ and $^{93}Nb(n,2n)^{92m}Nb$ reaction rate, and a fission chamber was used as a relative flux monitor. The average neutron flux at the irradiation position was about $5\times10^{5}$ n/cm$^{2}$/s. Samples were metals of natural abundance with 1.5 cm in diameter and 1 cm in thickness. Purity of the samples was more than 99.9%. Gamma-rays produced by interactions of neutrons with the samples were detected by an anti-compton spectrometer consisting of a HPGe detector and a BGO scintillation counter, which reduced compton continuum by high energy gamma-rays. The HPGe detector was placed at 29.6 cm from the sample with an angle of 90 degree with respect to the axis of the neutron beam. Detected gamma-ray peaks often contained prompt gamma-rays and decay gamma-rays. Decay gamma-rays were measured immediately after stop of the irradiation. They were subtracted from the total gamma-rays measured during the irradiation. Target materials, measurement times and principal gamma-rays are shown in Table 1.

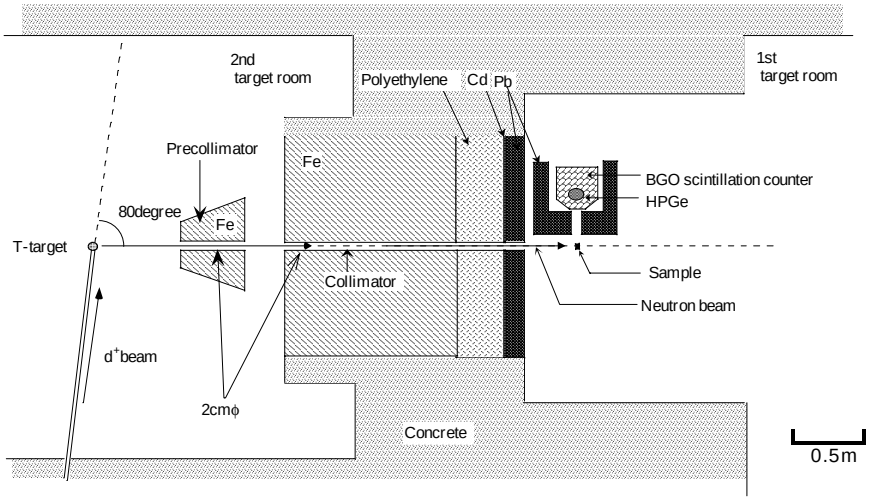


Fig. 1 The experimental arrengement (horizontal cross section).

Table 1 Target materials, measurement times and principal gamma-rays detected.

| Material | Measurement time(sec) | Major gamma-ray |
|---|---|---|
| Mg | 36000 | 90.993(Mg(n,xpγ)),1368.633(Mg(n,xγ) |
| Al | 33910 | 472.202($^{27}$Al(n,nαγ)), 843.7($^{27}$Al(n,n'γ)) |
| Si | 36679 | 1778.7($^{28}$Si(n,n'γ)), 2838.67($^{28}$Si(n,n'γ)) |
| Ti | 35410 | 983.517(Ti(n,xγ)) |
| Fe | 35278 | 846.8(Fe(n,xγ)), 1238.282(Fe(n,xγ)) |
| Ni | 36781 | 1332.5(Ni(n,xγ)), 1454.45($^{58}$Ni(n,n'γ)) |
| Cu | 35493 | 962.06($^{63}$Cu(n,n'γ)) |
| Nb | 23216 | 357.49($^{93}$Nb(n,2nγ)) |
| Mo | 31313 | 787.374(Mo(n,xγ)) |
| Ta | 36000 | 482.182($^{181}$Ta(n,n'γ)) |

3 Experimental Results and Discussion

Figure 2 and Table 2 show a gamma-ray spectrum for the Fe(n,xγ) reaction and the cross section data, respectively. The structure of Table 2 is following. Figure 3 shows ratios of cross section data for Fe target previously reported to the present data. In the case of intense gamma-rays, good agreements were showed among those data, but in the case of weak gamma-rays, large discrepancies were found among those data. Discrepancies between the present and previous data could be mainly due to the poor energy resolution of NaI(Tl) detectors or the poor counting statistics with use of the pulsed neutron sources. The data of Hlavac, which were systematically measured by using of the pulsed neutron, were in good agreement with the present data.

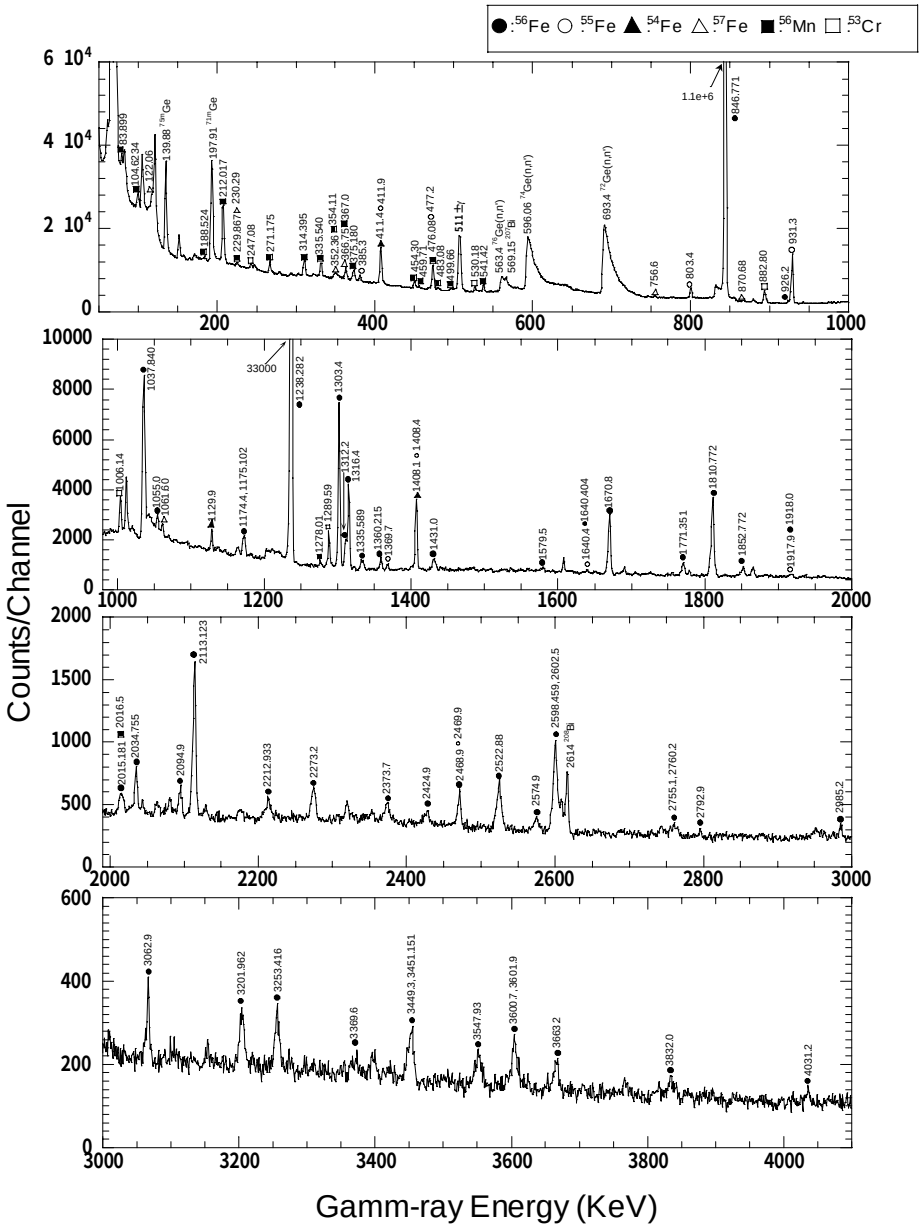


Fig. 2 Gamma-ray spectrum for Fe target at En=14.2 MeV.

Table 2(1/2) Measured discrete gamma-ray production cross section(preliminary)
Column 1- producing reaction; 2 - decay scheme (initial and final levels, their spins and parities); 3 - energy of gamma-ray in keV; 4 – experimental cross section in mb/sr; 5- error of data.

| Reaction | Transition | E $\gamma$ (keV) | d $\sigma$ /d $\Omega$ (mb/sr) | error(%) |
|---|---|---|---|---|
| Fe(n,p+np)$^{56}$Mn | 111(1+) → 27(2+) | 83.899 | 1.1 | 7 |
| Fe(n,p+np)$^{56}$Mn | 215(1+,2+) → 111(1+) | 104.6243 | 0.8 | 9 |
| Fe(n,n'+2n)$^{57}$Fe | 136(5/2−) → 14(3/2−) | 122.06 | 1.5 | 7 |
| Fe(n,p+np)$^{56}$Mn | 215(1+,2+) → 27(2+) | 188.524 | 0.2 | 20 |
| Fe(n,p+np)$^{56}$Mn | 212(4+) → 0(3+) | 212.017 | 3.2 | 5 |
| Fe(n,p+np)$^{56}$Mn | 716 → 486(3+) | 229.867 | 0.3 | 19 |
| Fe(n,n'+2n)$^{57}$Fe | 367(3/2−) → 136(5/2−) | 230.29 | | |
| $^{56}$Fe(n,$\alpha$)$^{53}$Cr | 1537(7/2−) → 0(3/2−) | 247.08 | 0.2 | 19 |
| Fe(n,p+np)$^{56}$Mn | 486(3+) → 215(1+,2+) | 271.175 | 0.7 | 8 |
| Fe(n,p+np)$^{56}$Mn | 341(3+) → 27(2+) | 314.395 | 0.8 | 9 |
| Fe(n,p+np)$^{56}$Mn | 336(5+) → 0(3+) | 335.54 | 0.8 | 8 |
| Fe(n,n'+2n)$^{57}$Fe | 367(3/2−) → 14(3/2−) | 352.36 | 0.5 | 15 |
| Fe(n,p+np)$^{56}$Mn | 840 → 486(3+) | 354.11 | 0.2 | 32 |
| Fe(n,n'+2n)$^{57}$Fe | 367(3/2−) → 0(1/2−) | 366.75 | 0.6 | 8 |
| | 3756(6+) → 3388(6+) | 367 | | |
| Fe(n,p+np)$^{56}$Mn | 716 → 341(3+) | 375.18 | 1.0 | 7 |
| $^{56}$Fe(n,2n)$^{55}$Fe | 1317(7/2−) → 931(5/2−) | 385.3 | 0.4 | 11 |
| $^{54}$Fe(n,n')$^{54}$Fe | 2949(6+) → 2538(4+) | 411.4 | 2.9 | 6 |
| $^{56}$Fe(n,2n)$^{55}$Fe | 411(1/2−) → 0(3/2−) | 411.9 | | |
| Fe(n,p+np)$^{56}$Mn | 454(3+9 → 0(2+) | 454.3 | 0.4 | 11 |
| Fe(n,p+np)$^{56}$Mn | 486(3+) → 27(2+) | 459.71 | 0.1 | 28 |
| Fe(n,p+np)$^{56}$Mn | 1192(4+) → 716 | 476.08 | 2.1 | 6 |
| $^{56}$Fe(n,2n)$^{55}$Fe | 1408(7/2−) → 931(5/2−) | 477.2 | | |
| Fe(n,p+np)$^{56}$Mn | 1237 → 753(3+) | 483.08 | 0.1 | 33 |
| Fe(n,p+np)$^{56}$Mn | 840 → 341(3+) | 499.66 | 0.1 | 35 |
| $^{56}$Fe(n,$\alpha$)$^{53}$Cr | 1537(7/2−) → 1006(5/2−) | 530.18 | 0.4 | 12 |
| Fe(n,p+np)$^{56}$Mn | 753(3+) → 212(4+) | 541.42 | 0.7 | 9 |
| $^{56}$Fe(n,$\alpha$)$^{53}$Cr | 564(1/2−) → 0(3/2−) | 564.3 | 0.8 | 10 |
| $^{54}$Fe(n,n')$^{54}$Fe | 3295(4+) → 2538(4+) | 756.6 | 5.3 | 17 |
| $^{56}$Fe(n,2n)$^{55}$Fe | 2212(9/2−) → 1408(7/2−) | 803.4 | 1.0 | 14 |
| Fe(n,n'+2n)$^{56}$Fe | 847(2+) → 0(0+) | 846.771 | 49.4 | 7 |
| Fe(n,n'+2n)$^{57}$Fe | 1007(7/2−) → 136(5/2−) | 870.68 | 0.3 | 24 |
| $^{56}$Fe(n,$\alpha$)$^{53}$Cr | 2172(11/2−) → 1290(7/2−) | 882.8 | 0.6 | 12 |
| $^{56}$Fe(n,2n)$^{55}$Fe | 931(5/2−) → 0(3/2−) | 931.3 | 7.9 | 5 |
| $^{56}$Fe(n,$\alpha$)$^{53}$Cr | 1006(5/2−) → 0(3/2−) | 1006.14 | 1.2 | 8 |
| Fe(n,n'+2n)$^{56}$Fe | 3123(4+) → 2085(4+) | 1037.84 | 5.5 | 9 |
| Fe(n,n'+2n)$^{56}$Fe | 4887 → 3832(2+) | 1055 | 0.8 | 23 |
| Fe(n,n'+2n)$^{57}$Fe | 1198(9/2−) → 136(5/2−) | 1061.6 | 0.0 | 27 |
| $^{54}$Fe(n,n')$^{54}$Fe | 2538(4+) → 1408(2+) | 1129.9 | 8.2 | 13 |
| Fe(n,n'+2n)$^{56}$Fe | 3832(2+) → 2658(2+) | 1174.4 | 0.9 | 28 |
| | 4298(4+) → 3123(4+) | 1175.102 | | |
| Fe(n,n'+2n)$^{56}$Fe | 2085(4+) → 847(2+) | 1238.282 | 27.3 | 5 |
| Fe(n,p+np)$^{56}$Mn | 1613 → 336(5+) | 1278.01 | 0.2 | 22 |
| $^{56}$Fe(n,$\alpha$)$^{53}$Cr | 1290(7/2−) → 0(3/2−) | 1289.59 | 1.4 | 7 |
| Fe(n,n'+2n)$^{56}$Fe | 3388(6+) → 2085(4+) | 1303.4 | 5.7 | 5 |
| Fe(n,n'+2n)$^{56}$Fe | 4701(7+) → 3388(6+) | 1312.2 | 1.0 | 8 |
| $^{56}$Fe(n,2n)$^{55}$Fe | 1317(7/2−) → 0(3/2−) | 1316.4 | 3.1 | 6 |
| Fe(n,n'+2n)$^{56}$Fe | 4459(4+) → 3123(4+) | 1335.589 | 0.5 | 26 |

Table 2(1/2) Measured discrete gamma-ray production cross section(preliminary)

| Reaction | Transition | E $\gamma$ (keV) | d $\sigma$ /d $\Omega$ (mb/sr) | error(%) |
|---|---|---|---|---|
| Fe(n,n'+2n)$^{56}$Fe | 3445(3+) → 2085(4+) | 1360.215 | 0.6 | 11 |
| $^{56}$Fe(n,2n)$^{55}$Fe | 2301(9/2) → 931(5/2−) | 1369.7 | 0.3 | 20 |
| $^{54}$Fe(n,n')$^{54}$Fe | 1408(2+) → 0(0+) | 1408.1 | 2.8 | 6 |
| $^{56}$Fe(n,2n)$^{55}$Fe | 1408(7/2−) → 0(3/2−) | 1408.4 | | |
| Fe(n,n'+2n)$^{56}$Fe | 4554(2+,3+,4+) → 3123(4+) | 1431 | 0.7 | 11 |
| Fe(n,n'+2n)$^{56}$Fe | 4540(1+,2+) → 2960(2+) | 1579.5 | 0.2 | 25 |
| $^{56}$Fe(n,2n)$^{55}$Fe | 2052(3/2−) → 411(1/2−) | 1640.4 | 0.2 | 30 |
| Fe(n,n'+2n)$^{56}$Fe | 4298(4+) → 2658(2+) | 1640.404 | | |
| Fe(n,n'+2n)$^{56}$Fe | 3756(6+) → 2085(4+) | 1670.8 | 3.4 | 6 |
| Fe(n,n'+2n)$^{56}$Fe | 3856(3+) → 2085(4+) | 1771.351 | 0.9 | 9 |
| Fe(n,n'+2n)$^{56}$Fe | 2658(2+) → 847(2+) | 1810.772 | 3.4 | 7 |
| Fe(n,n'+2n)$^{56}$Fe | 4510(3−) → 2658(2+) | 1852.4 | 0.6 | 13 |
| $^{56}$Fe(n,2n)$^{55}$Fe | 1918(1/2−) → 0(3/2−) | 1917.9 | 0.2 | 21 |
| Fe(n,n'+2n)$^{56}$Fe | 4878(2+) → 2960(2+) | 1918 | | |
| Fe(n,n'+2n)$^{56}$Fe | 4100(4+) → 2085(4+) | 2015.2 | 0.4 | 12 |
| Fe(n,p+np)$^{56}$Mn | 2016(2+) → 0(3+) | 2016.5 | | |
| Fe(n,n'+2n)$^{56}$Fe | 4120(3+) → 2085(4+) | 2034.755 | 0.5 | 14 |
| Fe(n,n'+2n)$^{56}$Fe | 2942(0+) → 847(2+) | 2094.9 | 0.5 | 15 |
| Fe(n,n'+2n)$^{56}$Fe | 2960(2+) → 847(2+) | 2113.123 | 1.4 | 10 |
| Fe(n,n'+2n)$^{56}$Fe | 4298(4+) → 2085(4+) | 2212.933 | 0.5 | 18 |
| Fe(n,n'+2n)$^{56}$Fe | 3120(1,2) → 847(2+) | 2273.2 | 0.8 | 11 |
| Fe(n,n'+2n)$^{56}$Fe | 4459(4+) → 2085(4+) | 2373.7 | 0.6 | 22 |
| Fe(n,n'+2n)$^{56}$Fe | 4510(3−) → 2085(4+) | 2424.9 | 0.4 | 26 |
| Fe(n,n'+2n)$^{56}$Fe | 4554(2+,3+,4+) → 2085(4+) | 2468.9 | 0.6 | 14 |
| $^{56}$Fe(n,2n)$^{55}$Fe | 2470(3/2−) → 0(3/2−) | 2469.9 | | |
| Fe(n,n'+2n)$^{56}$Fe | 3370(2+) → 847(2+) | 2522.88 | 1.5 | 29 |
| Fe(n,n'+2n)$^{56}$Fe | 4660(2+,3+,4+) → 2085(4+) | 2574.9 | 0.5 | 22 |
| Fe(n,n'+2n)$^{56}$Fe | 3445(3+) → 847(2+) | 2598.459 | 2.5 | 7 |
| | 3449(1,2) → 847(2+) | 2602.5 | | |
| Fe(n,n'+2n)$^{56}$Fe | 3602(2+) → 847(2+) | 2755.1 | 0.5 | 12 |
| | 3607(0) → 847(2+) | 2760.2 | | |
| Fe(n,n'+2n)$^{56}$Fe | 4878(2+) → 2085(4+) | 2792.9 | 0.2 | 26 |
| Fe(n,n'+2n)$^{56}$Fe | 3832(2+) → 847(2+) | 2985.2 | 0.3 | 24 |
| Fe(n,n'+2n)$^{56}$Fe | 5148 → 2085(4+) | 3062.9 | 0.7 | 15 |
| Fe(n,n'+2n)$^{56}$Fe | 4049(3+) → 847(2+) | 3201.962 | 3.7 | 10 |
| Fe(n,n'+2n)$^{56}$Fe | 4100(4+) → 847(2+) | 3253.416 | 0.6 | 17 |
| Fe(n,n'+2n)$^{56}$Fe | 3370(2+) → 0(0+) | 3369.6 | 0.4 | 20 |
| Fe(n,n'+2n)$^{56}$Fe | 3449(1,2) → 0(0+) | 3449.3 | 0.8 | 17 |
| | 4298(4+) → 847(2+) | 3451.151 | | |
| Fe(n,n'+2n)$^{56}$Fe | 4395(3+) → 847(2+) | 3547.93 | 0.9 | 11 |
| Fe(n,n'+2n)$^{56}$Fe | 4447.6 → 847(2+) | 3600.7 | 0.4 | 28 |
| | 3602(2+) → 0(0+) | 3601.9 | | |
| Fe(n,n'+2n)$^{56}$Fe | 4510(3−) → 847(2+) | 3663.2 | 0.7 | 11 |
| Fe(n,n'+2n)$^{56}$Fe | 3832(2+) → 0(0+) | 3832 | 0.5 | 16 |
| Fe(n,n'+2n)$^{56}$Fe | 4878(2+) → 847(2+) | 4031.2 | 0.2 | 36 |

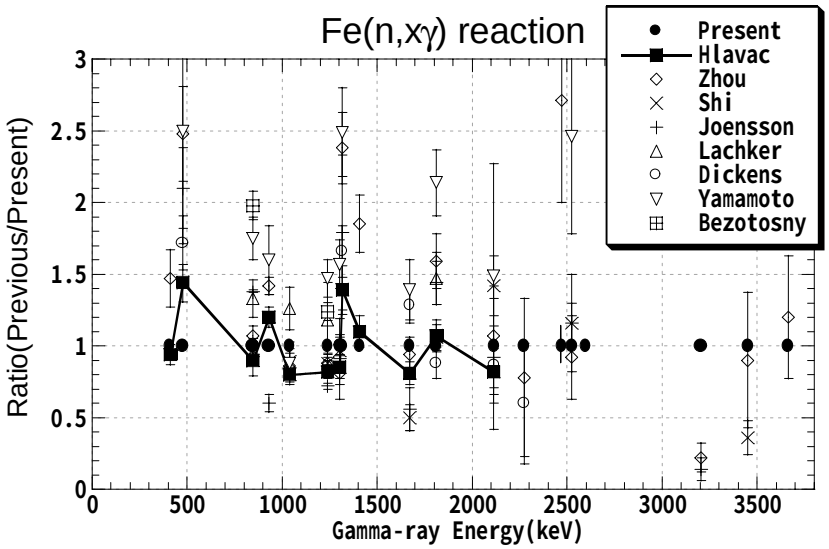


Fig. 3 The ratio of the previous cross sections to the present cross sections for the Fe(n,xγ) reaction with respect to gamma-ray energy.

4 Conclusion

Discrete gamma-ray production cross section data for Mg, Al, Si, Ti, Fe, Ni, Cu, Nb, Mo and Ta were obtained. Some cross section data for these targets are newly obtained. The data for Ta were obtained for the first time. The experimental efficiency obtained by the use of this system were about 50 times larger than the previous experiments using pulsed neutrons. Decay gamma-ray In result, good statistic data could bea obtained in a short span of time.

References

[1] S.P.Simakov et al.: "STATUS OF EXPERIMENTAL AND EVALUATED DATA FOR DISCRETE GAMMA-RAY PRODUCTION AT 14.5 MeV NEUTRON INCIDENT ENERGY", Report INDC(CCP)-413, IAEA (1998)